On the short-term response of entrained air bubbles in the upper ocean: a case study in the North Adriatic Sea

Benetazzo, A., Halsne, T., Bastianini, M., Breivik, O., Strand, K.O., Callaghan, A., Barbariol, F., Davison, S., Bergamasco, F., Molina, C

CNR ISMAR ISTITUTO DI SCIENZE MARINE

Meteorologisk institutt

Imperial College London

Università Ca'Foscari Venezia

NORTEK

Air **bubbles** in the upper ocean are generated mainly by wave **breaking** at the air-sea interface. As such, after the waves break, entrained air bubbles evolve in the form of **plumes** in the turbulent flow, **exchange gas** with the surrounding water, and may eventually rise to the surface. To shed light on the short-term response of entrained bubbles in different stormy conditions and to assess the link between bubble plume penetration depth, mechanical and thermal forcings, and air-sea transfer velocity of CO_2, a **field experiment** was conducted from an oceanographic research tower in the **North Adriatic Sea**. Air bubble plumes were observed using high-resolution **echosounder** data from an up-looking 1000-kHz sonar. The backscatter signal strength was sampled at a high resolution, 0.5 s in time and 2.5 cm along the vertical direction. Time series profiles of the bubble plume depth were established using a variable threshold procedure applied to the backscatter strength. The data show the occurrence of bubbles organised into **vertical plume-like structures**, drawn downwards by wave-generated turbulence and other near-surface circulations, and reaching the seabed at 17-m depth under strong forcing. We verify that bubble plumes adapt rapidly to wind and wave conditions and have depths that scale approximately linearly with **wind speed**. Scaling with the **wind/wave Reynolds number** is also proposed to account for the sea-state severity in the plume depth prediction. Results show a correlation between measured bubble depths and theoretical air-to-sea CO_2 transfer velocity parametrised with wind-only and wind/wave formulations. Further, our measurements corroborate previous results suggesting that the sinking of newly formed, **cold-water masses** helps bring bubbles to greater depths than those reached in stable conditions for the water column. The **temperature difference** between air and sea seems sufficient for describing this intensification at the leading order of magnitude. The results presented in this study are relevant for air-sea interaction studies and pave the way for progress in **CO_2 gas exchange formulations.**

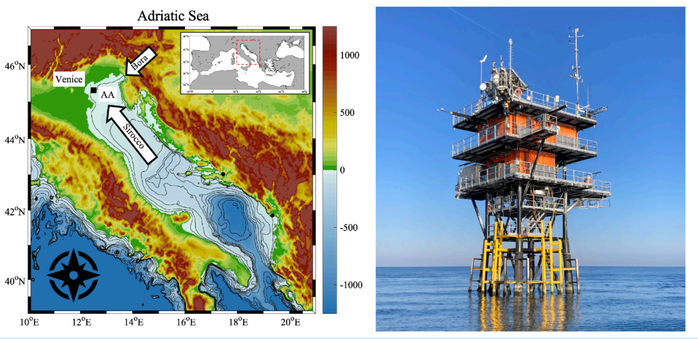

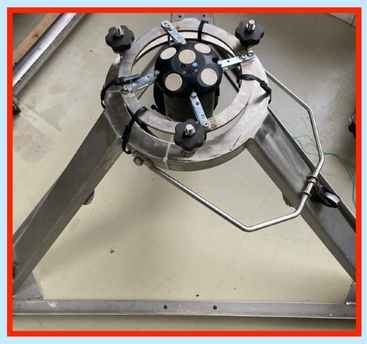

Observation of bubble plumes using a vertical-beam sonar

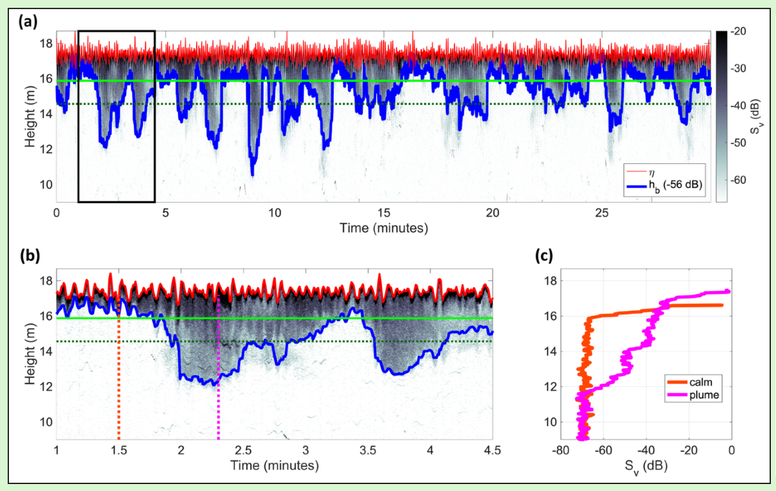

Example of measured air-bubble plume echo. The wind speed U_{10} was 8 m s^{-1} and the significant wave height H_s = 1.3 m. (a) Time-height volumetric backscatter strength S_v (grey shading, units in dB). Backscatter height (in meters) is measured upward from the sea bottom. Bubble plume height h_b (blue line; threshold level of -56 dB) and surface wave elevation (red line). The solid light-green and dashed dark-green lines show the depth H_s and 2 H_s, respectively. The solid black rectangle shows the echo chunk zoomed on panel b. (b) Zoom of the panel (a) between 1.0 and 4.5 minutes. (c) Vertical profiles (up to the air-sea interface) of backscatter strength during a calm period (dashed orange vertical transect in panel b) and within a bubble plume (dashed violet vertical transect in panel b).

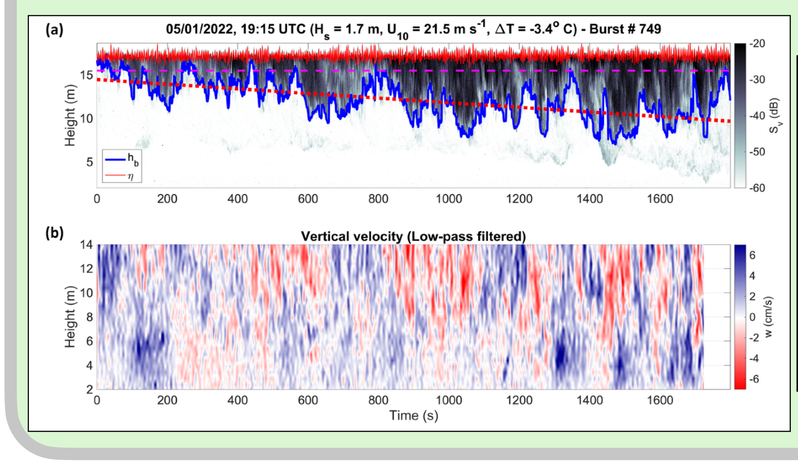

Response of the air-bubble plume at the onset of the cold-air outbreak on 5 January 2022. (a) Volumetric backscatter strength S_v is in grey shading (units in dB). Backscatter height (in meters) is measured upward from the sea bottom level. The bubble plume height is shown with a blue line and the surface wave elevation with a solid red line. The dashed magenta line shows the depth of H_s, and the dotted red line shows the line of best fit of the bubble depth. (b) The vertical component w of the residual velocity (units in cm/s; positive upward) after low-pass filtering w at 0.1 Hz.

Response and scales of bubble plumes

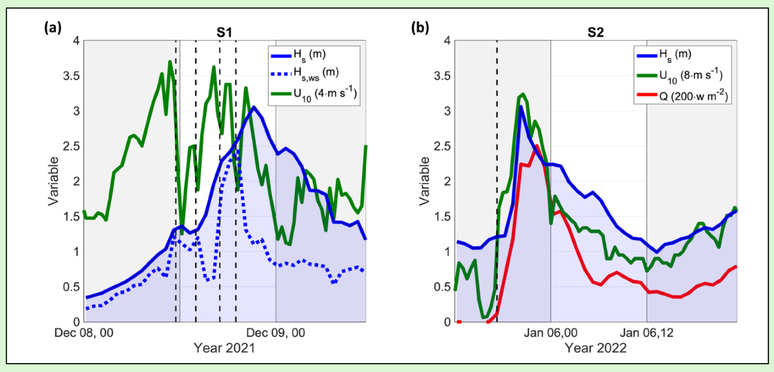

Atmosphere and wave conditions measured at the observation site. Variables: 10-m height average wind speed U_{10} (in meters per second), total significant wave height H_s (in meters), wind-sea significant wave height $H_{s,ws}$ (in meters), and heat flux Q (in W/m^2). Wind speed and heat flux are linearly scaled for graphical purposes with the coefficients provided in the legend. The dashed vertical black lines show the instant when the wind turned. (a) Mixed-sea storm on 8-9 December 2021. (b) Unimodal, cold-air storm on 5-6 January 2022.

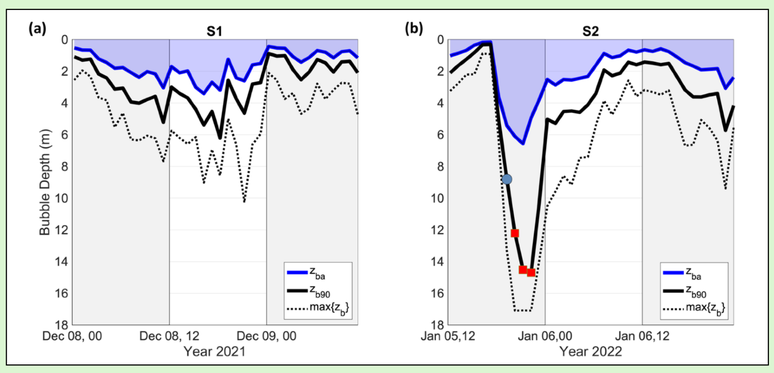

Time development of the bubble plume depth z_b during the two storms S1 (a) and S2 (b). Values of the average (z_{ba}; solid blue line) and 90th percentile (z_{b90}; solid black line) of the bubble depth. The dotted black line shows the maximum bubble depth max{z_b}. In panel b, the red markers show instants on the z_{b90} curve when the bubble plume reached the sonar head, and the blue-silver marker shows the instant at the onset of the cold-air outbreak.

Bubble plume penetration depth and surface forcings

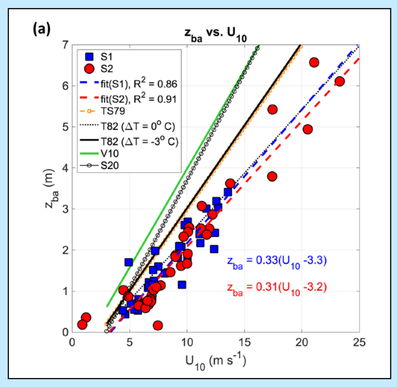

Relationship between bubble plume depth and wind parameters. Average bubble penetration depth z_{ba} versus 10-m height wind speed U_{10} (a) and friction velocity (b). Empirical data over storms S1 (blue marker) and S2 (red marker) and lines of best fit (dashed curve; equations in the plot area with the same colour code). Reference curves: TS79 (marked orange line), Thorpe and Stubbs (1979); T82 (DT = 0° C) (dotted black line), Thorpe (1982) with air-water temperature difference DT = 0° C; T82 (DT = -3° C) (solid black line), Thorpe (1982) with air-water temperature difference DT = -3° C (the mean temperature difference during storm S2); V10 (green line), Vagle et al. (2010); S20 (marked black line) is a fit of Strand et al. (2020) data.

Effect of dense-water formation

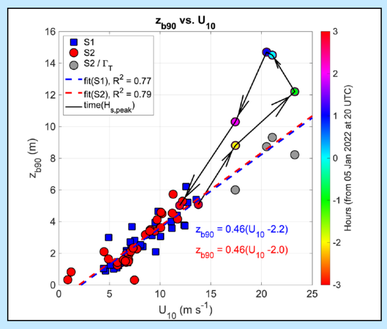

Relationship between 90th percentile of the bubble depth z_{b90} and 10-m height wind speed U_{10}. Empirical data from storms S1 (blue marker) and S2 (red marker) and lines of best fit (dashed curve; equations in the plot area with the same colour code). Colour-mapped markers and black arrow lines indicate values during S2 from -3 hours to +3 hours across the peak of heat flux Q. Grey markers show the same points but corrected ($z_{b90,corr}$) with the stability parameter G_T.

Scaling with wind and waves

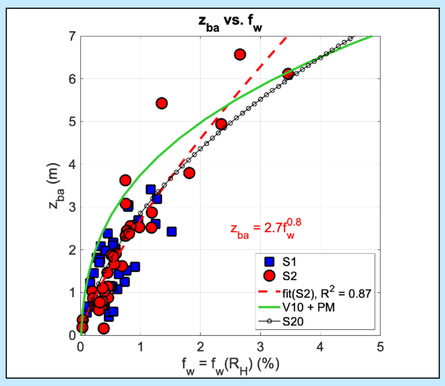

Bubble Depth and CO_2 Transfer Velocity

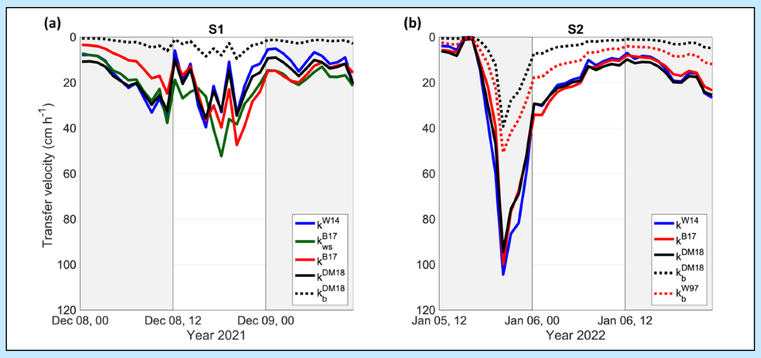

Time history of theoretical gas transfer velocity of CO_2 during storms S1 (a) and S2 (b). Theoretical estimates of the total velocity k according to parametrisations by Wanninkhof 2014 (solid blue line), Brumer et al. 2017 (solid red and solid green lines, respectively), and Deike&Melville 2018 (solid black line). Theoretical estimates of the bubble-mediated contribution to k according to parametrisations by Deike&Melville 2018 (dotted black line) and Woolf 1997 (dotted red line).

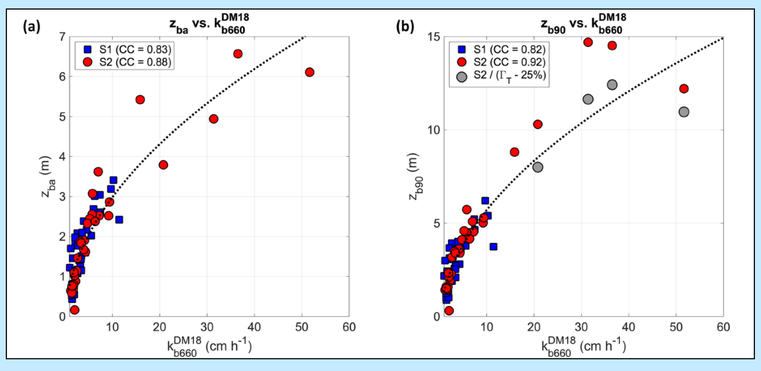

Relationship between bubble-mediated parametrization of CO_2 gas transfer velocity and average (a) and 90th percentile (b) bubble depths. Data from storms S1 (blue marker) and S2 (red marker) and curve of best fit for S1 and S2 data aggregated (dotted black curve; equation in the plot area). Grey markers indicate values across the peak of heat flux Q during S2 corrected with the stability parameter G_T reduced empirically by 25%.

Conclusions

The main observational findings and inference of the study are summarized as follows:

Shallow and deep bubble plumes demonstrate a **short-time response and direct connection with the surface forcings**. In line with previous studies that analysed the bubble penetration depths in the ocean, we have found that bubble penetrations follow an empirical linear law with wind speed closely, although the difference in the wind-speed regime and wave development between the two storms focus of this study. **The minimum wind speed for bubble plumes to be generated is around 3 m s^{-1}.** When compared with previous parametrisations of the same type, data display smaller penetration depths for a given wind speed, which we considered as being due to the limited growth of waves in the North Adriatic Sea. When the wave forcing is incorporated in the assessment using a **scaling with the wind/wave Reynolds number**, a reconciliation between data sets collected at different locations and sea-state severity seems plausible.

During the second storm (S2) focus of this study, we documented a large air-sea temperature difference that led to the **cooling of waters** and an intensification of the **downward thermal convection**. Although it is not a new phenomenon to describe, we recognise that it strongly affects the larger bubble depths, whose enhancement can be parametrised at the leading order by the air-sea temperature difference. After being corrected for the **stability parameter proposed by Thorpe (1982)**, the bubble depth data reconciled with others measured during other phases of the same storm and those from the first storm (S1) when heat fluxes were small.

During the intense heat-flux phase of the second storm (S2), the **bubble plume reached the seabed (17 m) and its depth exceeded 6H_s**; otherwise, the maximum depths were at about half of the water column. The bubble depths followed a Lognormal distribution, suggesting that a set of independent forces are at play simultaneously that determine the depths reached by the bubbles. However, the used sonar did not permit separating the contributions from different sources. Deeper and denser bubble plumes were accompanied by **vertical convection with a downward maximum speed of 7 cm s^{-1}**.

The t**ransfer velocity k of CO_2 gas was estimated** from measured data using wind-only and wind/wave semi-empirical parameterisations. During the two storms S1 and S2, values of k reached 40 cm h^{-1} and 100 cm h^{-1}, respectively, with small differences between predictions from the wind-dependent Wanninkhof (2014) model and the wind/wave-dependent Deike and Melville (2018) model. Differences from the latter exceeding 10 cm h^{-1} were found during S1 using the predictions of Brumer et al. (2017a). The bubble-mediated contribution to k was remarkable during S2, up to 40 cm h^{-1}, according to Deike and Melville (2018).

By using the penetration depth of bubble plumes as a proxy for the intensity of the surface processes (wind and waves), we found a s**trong correlation between plume depth and theoretical CO_2 transfer velocity**. This result was found for estimates of the total and the bubble-mediated contributions to k and for the average and extreme penetration depths, except for those values measured during the sinking of cold-water masses. In these conditions, the scaling of k with a stability parameter provides a possible means to include the thermal convection effects in the air-sea exchange of CO_2 gas. Results point in the direction that improved parameterisations of gas fluxes across the air-sea surface are needed to predict the future uptake of these gases by the oceans.

Reference: https://doi.org/10.5194/egusphere-2023-2387